Arch. Metall. Mater. **63** (2018), 3, 1209-1215

DOI: 10.24425/123793

A. WOŹNIAK*#, B. ZIĘBOWICZ*, A. ZIĘBOWICZ**, W. WALKE**

PHYSICOCHEMICAL PROPERTIES OF OXIDE ZrO_2 LAYER DEPOSITED BY SOL-GEL METHOD ON Ti-6Al-7Nb ALLOY

The paper contains the results of the initial surface treatment influence on the properties of the medical Ti-6Al-7Nb alloy with a modified zirconium oxide layer deposited on its surface by sol-gel method. In the paper, the analysis of results of potentiodynamic studies is presented as well as its resistance to pitting corrosion and electrochemical impedance spectroscopy (EIS), macroscopic observation of the surface of samples and analysis of geometrical structure with the use Atomic Force Microscope (AFM) were performed. The studies were performed on two groups of samples depending on the graduation of the sand used in sandblasted process – 50 μm and 250 μm. Based on the obtained results it can be concluded that the type of the initial surface treatment preceding the surface modification of the Ti-6Al-7Nb has a significant effect on its properties.

Keywords: Titanium alloy; Sol-gel method; ZrO_2 layer; Corrosion test; AFM

1. Introduction

Currently, it was observed that the human population with disabilities within the musculoskeletal system and stomatoganthic system is going up and extending the lives in highly developed countries' societies at the same time. The musculoskeletal system insufficiency could cause injuries and lesion. Taking all these aspects into account, many scientists assess increase and summarize the knowledge of biomaterials, but also improve them and search for new solutions that guarantee optimal biotolernace in the tissue environment [1-6]. Currently, the vanadium-free Ti-6Al-7Nb alloy is one of the most popular and most prospective metal biomaterials used in medical and dental applications to made implants. The Ti-6Al-7Nb alloy characterizes in satisfactory mechanical properties, including value of Young's modulus of 105 GPa, which makes it a good material for cooperation with the bone. Additionally, this alloy is characterized by good corrosion resistance in human body solutions. Meanwhile, the unquestionable disadvantages of Ti-6Al-7Nb alloy is the existence of unsafe aluminum in its chemical composition. Included in the chemical composition aluminum can lead to nerve cell damage, allergy and osteomalacia, which is manifested as bone pain and frequently contributing to fractures. Additionally, the unstable passive surface layer and low tribological properties are limiting factors of the Ti-6Al-7Nb alloy usage in medical applications [5-9]. In order to eliminate unfavorable factors, it is necessary to use surface modification. Reports in the literature indicate that surface modification of Ti-6Al-7Nb alloy can be deposited on their surface thin oxide layer by sol-gel method have significantly effect on improving properties of this alloy. Usually the sol-gel method is used to applied single – and multi – component as well as multilayer coating. The oxide layer deposited by this method are characterized by control chemical composition and microstructure, which thickness exceeds the value 1 μm. Additionally, one of the advantages of sol–gel method is the possibility to create independently the hydroxyapatite on the deposited layers due to the interaction with the physiological fluid [9-13]. For this purpose, the zirconium oxide in one of the most popular layer used in sol-gel method. The ZrO_2 layer is characterized by good mechanical properties determined by high hardness, good bending strength and fracture toughness. In addition, it is distinguished by very good anticorrosion properties, which translates into its high biocompatibility.

2. Materials and methods

The subject of the research was Ti-6Al-7Nb alloy in form of disc of diameter $\phi = 14$ mm and thickness $d = 4$ mm (Forecreu SA), which chemical compositions met the requirements of the PN – EN ISO 5832 – 11 (Table 1) [14].

At first the samples were subjected to initial surface treatment including the mechanical grinding and sandblasting. The mechanical grinding was performed with the use abrasive SiC paper with the grain size of 120 grain/mm^2 (LabPOL – 25 by Struers). Later the samples were divided into two groups, depending on grain thickness of sand used in sandblasting process: first group – 50 μm (Ti6Al7Nb_50) and second group – 250 μm

* SILESIAN UNIVERSITY OF TECHNOLOGY, DIVISION OF BIOMEDICAL MATERIALS ENGINEERING, KONARSKIEGO 18A, 44-100 GLIWICE
** SILESIAN UNIVERSITY OF TECHNOLOGY, DEPARTMENT OF BIOMATERIALS AND MEDICAL DEVICES ENGINEERING, ROOSEVELTA 40, 41-800 ZABRZE
# Corresponding author: anna.wozniak@polsl.pl

TABLE 1

Chemical composition of Ti-6Al-7Nb alloy

	Elements, [% wt]								
	Al	**Nb**	**Ta**	**Fe**	**O**	**C**	**N**	**H**	**Ti**
Certificate	5.70	6.70	0.44	0.18	0.16	0.04	0.02	0.007	rest
ISO 5832 – 11	6.00	7.00	>1.20	>0.20	>0.18	>0.05	>0.04	>0.008	rest

(Ti6Al7Nb_250). The sandblasting (MICRA 2 by Dentalfarm) was carried out with the use synthetic Al_2O_3 at a pressure of 3 bar. In the next stage a zirconia oxide layer was deposited on the surface of tested samples by sol-gel method. The process was carried out in the atmosphere of nitrogen being an inert gas. The reaction substrates were infused in several stages (Fig. 1), each time terminating with thorough mixing of the solution with speed of 300-600 rpm with the use magnetic stirrer (CAT EXM 6). As the zirconium oxide precursor zirconium isopropoxide $Zr(OC_3H_7)_4$ was used, which, because of the high electric charge, was introduced into the reactor first and then stabilized. After stabilization, the speed of magnetic stirrer 2-propanol was added and the solution was stirred for 15 minutes. In the next step the inhibitor – acetylacetone $C_5H_8O_2$, was added as a chelating agent to the reaction vessel. After 45 minutes of stirring, yttrium nitrate $Y(NO_3)_3$ x $6H_2O$ was added as an yttrium precursor. At last the distilled water and 2-propanol was dosed to the solution using the "drop by drop" method, until a homogeneous gel of modified zirconium oxide with a chemical composition of 98% ZrO_2 + 2% Y_2O_3 was obtained.

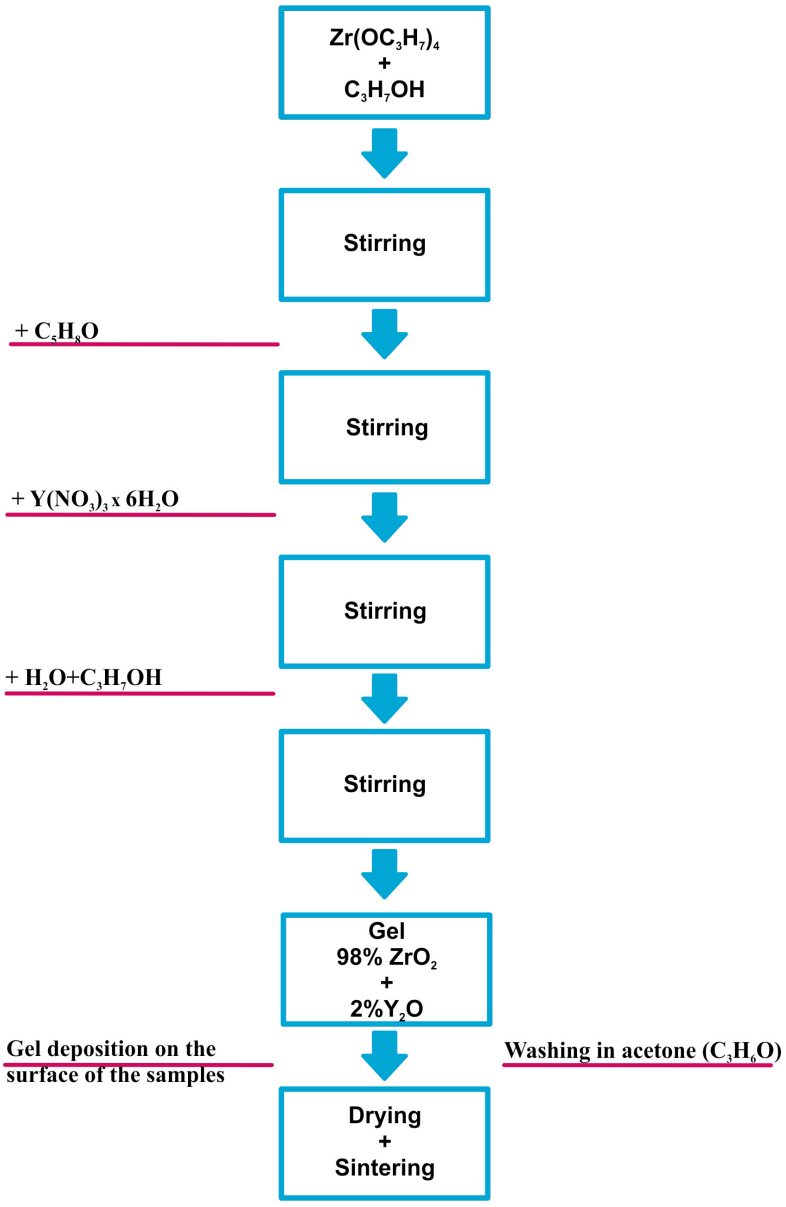

Fig. 1. Sol-gel etaps

The obtained ZrO_2 layer was deposited on the surface of the tested samples with the use immersion method (Fig. 2). The samples were immersed in the sol by hand.

Following the samples with the ZrO_2 gel were subjected to the heat treating (Refter Magme). The samples were baked at an initial temperature $T = 50°C$ for time $t = 60$ min. Then the temperature was increased to $T = 100°C$ and the samples were baked for $t = 120$ minute. The heating rate was equal to $V = 5°C/min$.

The aim of the research was to determine the most favorable method of the initial surface treatment, preceding the deposition on the surface of the dental alloy Ti-6Al-7Nb modified zirconium oxide layer by sol-gel method.

2.1. Electrochemical impedance spectroscopy

In order to determine the physicochemical properties of tested samples the Electrochemical Impedance Spectroscopy (EIS) study was conducted. The study was carried out with the use of AutoLab's PGSTAT 302N measurement system equipped with the Frequency Response Analyser FRA2 module and the electrochemical cell with three-electrode system: working electrode (anode) – test sample, the auxiliary electrode – platinum wire (PTP-201) and reference electrode – calomel electrode (SEC KP-113). The system allowed the tests to be carried out in the frequency range of 10^4-10^{-3} Hz and the voltage amplitude of sinusoidal signal actuating amounted to 10 mV. On the basis of the taken test the impedance system spectra in form of Nyquist diagrams and Bodes diagrams were determined. The obtained measurement data

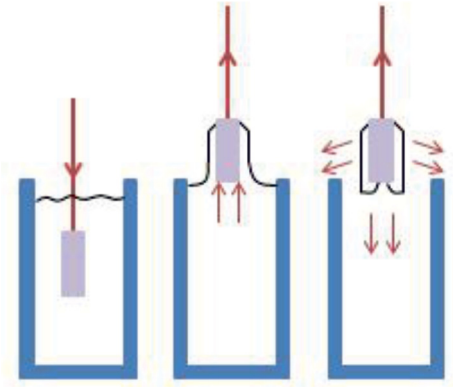

Fig. 2. Immersion method

were adjusted through the method of the smallest squares to the substitute setup and the values of resistance R and capacity C were determined. The researches were carried out in 250 ml Ringer solution (pH = 6.9 ± 0,2) at temperature $T = 37 \pm 1$°C. The chemical composition of Ringer solution are given in Table 2.

TABLE 2

Chemical composition of Ringer solution

Component	Quantity, [g/cm^3]
NaCl	8.60
KCl	0.30
$CaCl_2$ x $2H_2O$	0.33

2.2. Potentiodynamic polarization

In the next stage, in order to determine the resistance to pitting corrosion, the potentiodynamic tests were performed by recording the anodic polarization curves. For this purpose, the test stand included a VoltaLAB PGP201 potentiostat, computer with VoltaMaster 4 software and an electrochemical cell identical to that used in potentiodynami test. The anodic polarization curves were recorded from the initial potential $E_{int} = E_{ocp} - 100$ mV. The potential change was in the direction of the anodic at a rate of 1 mV/s. Once the anodic current density reached $i = 1$ mA/cm^2 or the potential reached the values $E = 4000$ mV, the polarization direction was changed and the return curves were recorded. On the basis of the recorded curves the values of characteristic parameter of the resistance to pitting corrosion were determined: corrosion potential E_{corr} [mV], potential of transpassivation E_{tr} [mV], polarization resistance R_p [kΩ · cm^2]. The corrosion current density was calculated from the formula $i_{corr} = 0.026/R_p$.The potentiodynamic polarization was carried out in identical conditions to the EIS test.

2.3. Macroscopic observation

In order to analyze the morphology of the tested alloys after potentiodynamic test was macroscopic observations of the surfaces which were conducted with the use of stereomicroscope SteREO Discovery.V8 produced by Zeiss in the10×-80× magnification rage.

2.4. Atomic force microscopy

In the next stage in order to obtain additional information on surface topography of the tested samples microscopic observation with the use Atomic Force Microscopy was performed. The observation was performed with the use XE-100 microscope by Park System with a non-contact mode. The parameter describing the surface roughness – the arithmetic average of ordinates profile (R_a) was calculated over three scan area 25×25 μm.

3. Results

3.1. Electrochemical impedance spectroscopy

The obtained results in form of impedance spectra were presented in Figs. 3 and 4. On the basis of the recorded diagram the values of characteristic electric parameters were determined

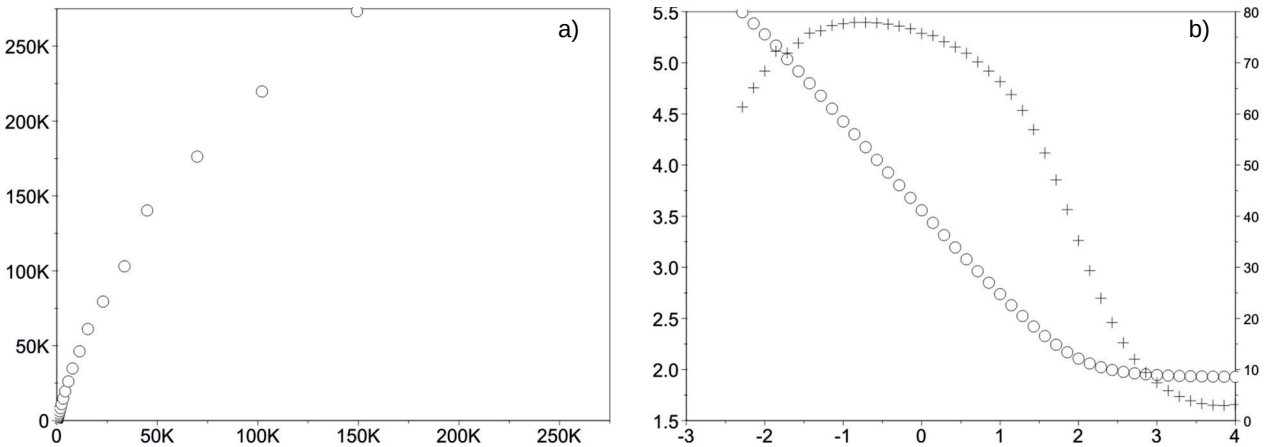

Fig. 3. Sample spectra impedance for Ti6Al7Nb_50 samples with ZrO2 layer: a) Nyquist diagram, b) Bode's diagram

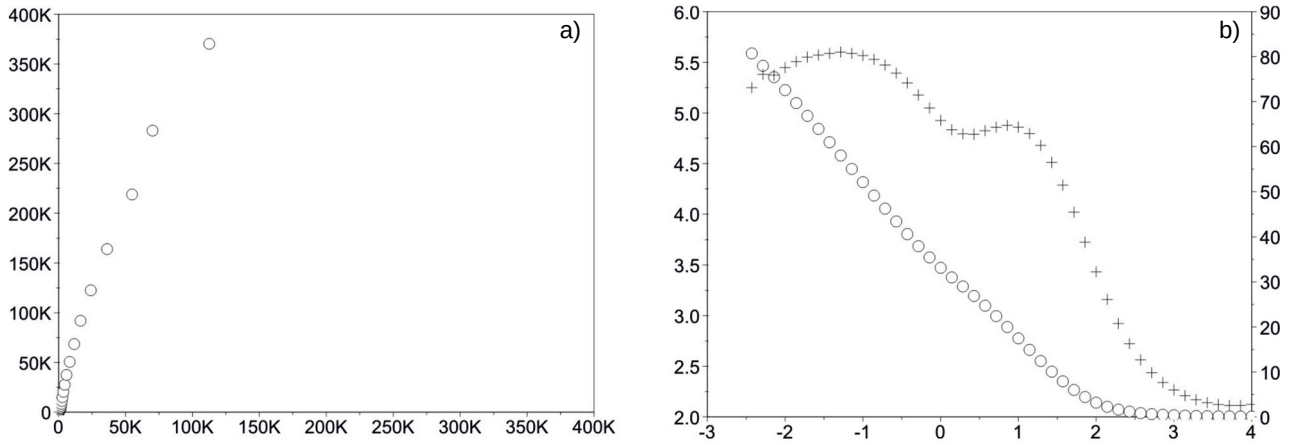

Fig. 4. Sample spectra impedance for Ti6Al7Nb_250 samples with ZrO2 layer: a) Nyquist diagram, b) Bode's diagram

(Table 3) and the equivalent circuits were proposed. It was found that for both groups of the tested alloys, the best fit of the model spectra to the impedance spectra is provided by equivalent circuits composed of two parallel electric elements representing capacitive or constants CPE of border combined with resistance transitions and resistance R (Fig. 5). For equivalent circuits designations, it stands out: R_{ct} – resistance of the charge transition at phases border, CPE_{dl} – capacity of oxide layer, R_{pore} – resistance of electrolyte in porous phase, CPE_{pore} – capacity of porous layer and R_s – resistance recorded at high frequencies (artificial saliva solution). The obtained equivalent circuits is characteristic for the double layer, which consisting of an internal oxide layer ($CPDE_{dl}$ and R_{ct}) and an outer, porous layer (CPE_{pore} and R_{pore}).

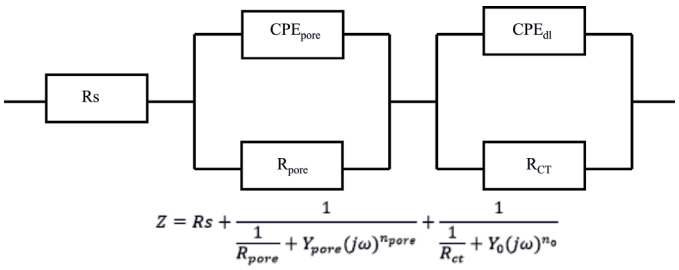

Fig. 5. Electric substitute schemes

The Nyquist diagrams for the both Ti6Al7Nb_50 samples and Ti6Al7Nb_250 samples presented of fragments of incomplete semicircles, which was a typical impedance response for an oxide thin layer. For the samples blasted using grain size of 250 μm compared to the samples blasted with the use grain size of 50 μm, bigger radius of the semicircles was recorded. It indicates a better corrosion resistance of Ti6Al7Nb samples, which was independently corroborated by values of R_{ct} resistance (it determines corrosion rate). The mean value of R_{ct} resistance for Ti6Al7Nb_250 samples was $R_{ct} = 2236$ kΩcm^2 and it was double or even more than the value of R_{ct} resistance for Ti6Al7Nb_50 samples, for which the average value was $R_{ct} = 1015$ kΩcm^2. The maximum values of phase displacement at a broad range of frequencies presented in the Bode diagrams for the both groups of samples were similar and amounted to approximately $\theta = 80°$. Additionally, for both variants of samples, the inclinations log|Z| at the whole scope of frequency change are close to –1 which indicates the capacity character of porous layer. The similar results for the sandblasted samples of Ti6Al7Nb alloy were obtained, where the impedance characteristics have the typical shape for the presence of an oxide layer [15].

3.2. Potentiodynamic polarization

The results of potentiodynamic test indicate to different corrosion resistance of Ti6Al7Nb_50 and Ti6Al7Nb_250 samples. The recorded anodic polarization curves were presented in Figs. 6 and 7, and the characteristic values describing corrosion resistance were given in Table 4.

The obtained progress of the polarization curves for the both Ti6AlNb_50 samples and Ti6Al7Nb_250 samples were similar and no existence of histories loops were recorded – the progress of curves were characteristic for material with a high corrosion resistance. For the Ti6Al7Nb_250 samples the existence of transspasivation potential E_{tr} has been stated, which mean value was $E_{tr} = +1474$ mV. Meanwhile, for the Ti6Al7Nb_50 samples

TABLE 3

EIS results

Sample	E_{ocp}, [mV]	R_s, [Ωcm^2]	R_{pore}, [kΩcm^2]	CPE_{pore}		R_{st}, [kΩcm^2]	CPE_{dl}	
				Y [Ω^{-1} cm^{-n}s^{-n}]	n		Y [Ω^{-1} cm^{-n}s^{-n}]	n
Ti6Al7Nb_50	–140	99	146	0,756E–3	0,68	1015	0,565E–4	0,88
Ti5Al7Nb_250	–176	100	100	0,895E–4	0,87	2236	0,756E–4	0,92

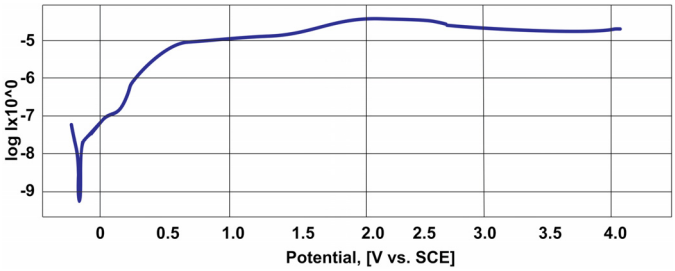

Fig. 6. Example of polarization curves for Ti6Al7Nb_50 samples

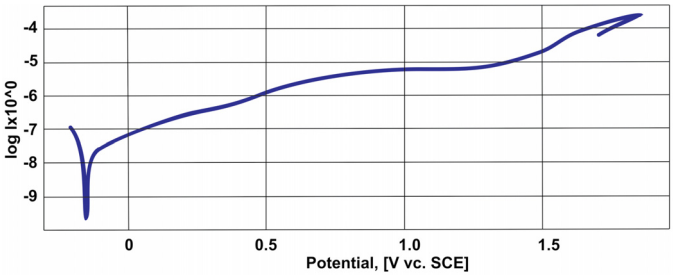

Fig. 7. Example of polarization curves for Ti6Al7Nb_250 samples

TABLE 4

Results of potentiodynamic tets

Sample	E_{init}, [mV]	E_{corr}, [mV]	E_{tr}, [mV]	R_p, [MΩ/cm^2]	i_{corr}, [µA]
Ti6Al7Nb_50	–100	–182	—	0.82	0.032
Ti5Al7Nb_250	–90	–154	+ 1474	1.28	0.020

demonstrates total resistance to pitting corrosion the polarization potential scope up to the range of E = +4V. The mean value of pitting corrosion potential for Ti6Al7Nb_50 samples was –182 mV and it was higher corporate to values recorded for the Ti6Al7Nb_250 samples, which the average value was –154 mV. A similar relationship was observed in case of polarization resistance values, which for Ti6Al7Nb_50 and Ti6Al7Nb_250 samples amount to 0.82 MΩcm^2 and 1.28 MΩcm^2, respectively. For the only sandblasted samples [15] the mean value of pitting corrosion resistance was E_{corr} = –350 mV and it was the lowest value compared to the value of E_{corr} obtained for the sandblasted samples with ZrO_2 layer.

3.3. Macroscopic observation

The results of macroscopic observation of samples in initial state and Ti6Al7Nb_50, Ti6Al7Nb_250 samples with deposited ZrO_2 layer before electrochemical test indicate a significant differences of surface topography. The surface of the samples in initial state was characterized by stratches, which is the result of mechanical treatment. The sandblasting process makes it possible to increase the repeatability of the surface. The surface of the samples blasted with the use grain size 50 µm was characterized by the largest surface development in comparative to the samples Ti6Al7Nb_250 and the samples in initial sate. Additionally, it was found that the ZrO_2 layer on the surface of the Ti6Al7Nb_50 and Ti6Al7Nb_250 samples was inhomogeneous – the microcracks were formed during backed [12]. Meanwhile, based on observation of the surface of the tested samples shown that the electrochemical study does not have a significant effect on the quality of their surface (Fig. 8).

3.4. AFM

AFM observation results of the tested samples with the deposited ZrO_2 layer and in initial state were presented in Figs. 9, 10 and 11. The highest values of the surface roughness parameter R_a was recorded for the Ti6Al7Nb_50 sample, which mean value as R_a = 0.536 µm. For the sample blasted with the use 250 µm grain size the average value was R_a = 0.488 µm, meanwhile for the sample in initial state R_a = 0.096 µm. Based on obtained results, it was found that the type of the surface modification and initial surface treatment significantly affects the quality of the surface topography. Additionally, in case of the Ti6Al7Nb_50 and Ti6Al7Nb_250 samples, the ZrO_2 layer reconstructed the topography of the samples after sandblasted. On the basis on the obtained results and conclusion from paper [20], it can be concluded that, the ZrO_2 layer could reconstructed the topography of the sandblasted samples. The mean value of AFM roughness of sandblasted samples was 0,32 µm.

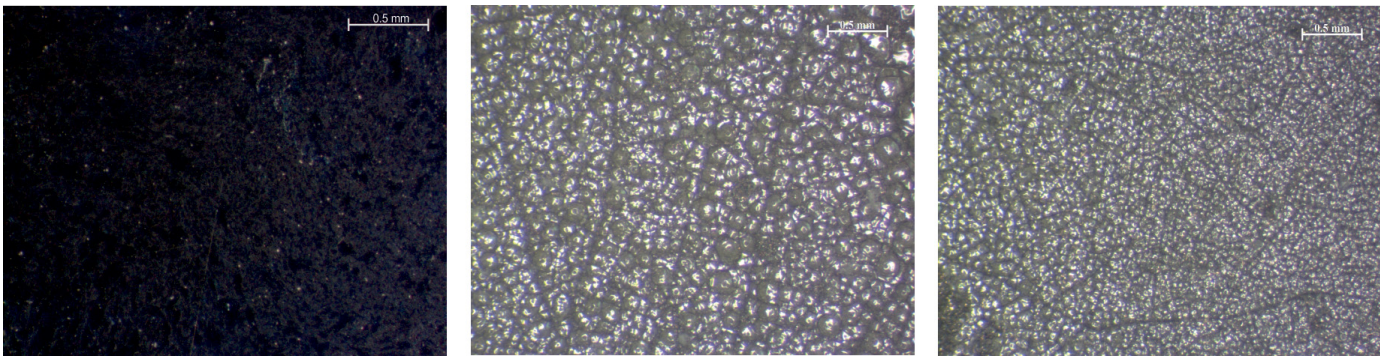

a) b) c)

Fig. 8. Macroscopic observation of a) Ti6Al7Nb_inital state, b) Ti6Al7Nb_50, c) Ti6Al7Nb_250

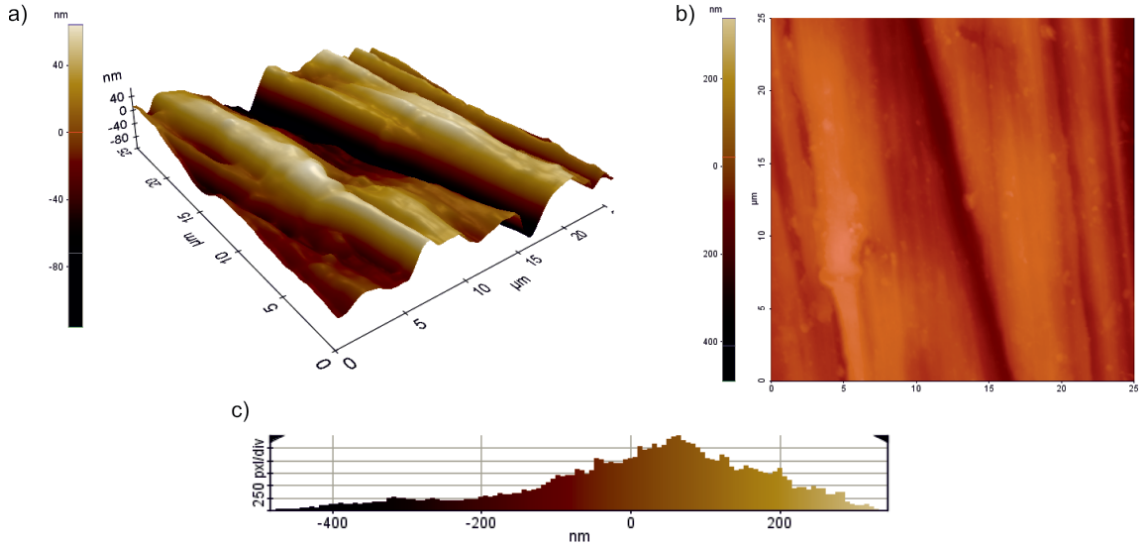

Fig. 9. AFM results Ti6Al7Nb in initial state

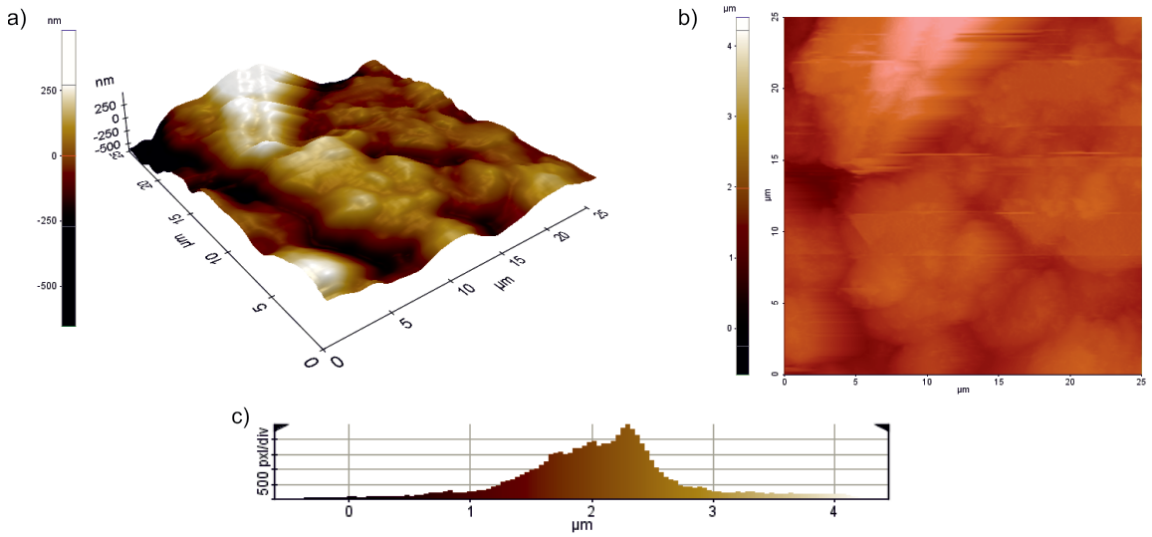

Fig. 10. AFM results Ti6Al7Nb_50

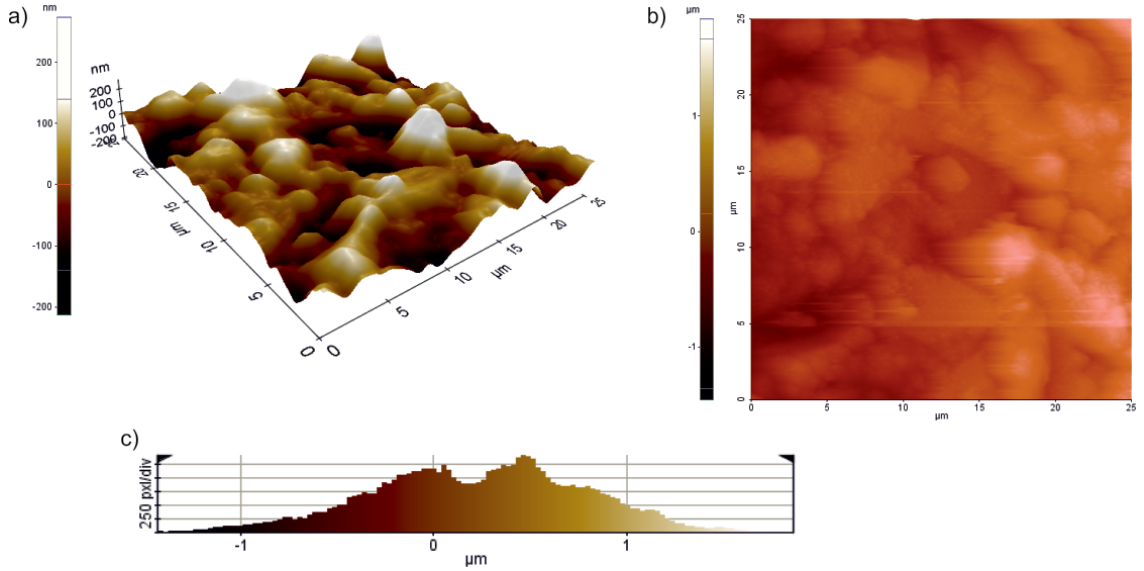

Fig. 11. AFM results Ti6Al7Nb_250

4. Conclusion

The analysis of the obtained results indicates the different pitting corrosion resistance of the Ti6Al7Nb_50 and Ti6Al7Nb_250 samples with deposited on their surface modified zirconium oxide layer. For the samples blasted with the use 250 μm grain size double or even more value of resistance of the charge transition at phases border R_{ct} comparted to the value for Ti6Al7Nb_50 samples was recorded. Based on the analysis of the polarization test, for Ti6Al7Nb_250 samples a higher values of the corrosion potential E_{corr}, the polarization resistance R_p and no change in the structure of the oxide layer on theirs surface were recorded. This is the result of the reconstruction of the oxide layer on the surface of the sample as a result of its polarization. The electrochemical tests showed that the type of the initial treatment the surface (before deposited the ZrO_2 layer) does a significant effect on the pitting corrosion resistance of the Ti-6Al-7Nb alloy. The use of the synthetic Al_2O_3 with a grain size 250 μm after the surface modification by the sol-gel method, results in obtaining a tight ZrO_2 layer, which is a good barrier against the corrosive environment. Additionally, based on the obtained results and literature dates it can be concluded, that the pitting corrosion resistance increase with the deposited on the surface of the Ti-6Al-7Nb alloy the thin layer by the sol-gel method [5,7,11]. Moreover, regardless of type of the initial surface treatment, the micro-crack of the oxide layer was observed, which does not affect the quality of the obtained layers. In the future, due to the increasing requirements for the quality of the biomaterials used in medical application, the use of the surface modification will be inevitable.

Acknowledgement

This work was supported by the Ministry of Science and Higher Education of Poland as the statutory financial grant of the Faculty of Mechanical Engineering, Silesian University of Technology.

REFERENCES

[1] K. Makuch, R. Koczorowski, Dent. & Med. Probl. **47** (1), 81-88 (2010).
[2] A. Zięty, M. Lachowicz, Aktual. Probl. Biomech. **4**, 143-145 (2014).
[3] B. Ziębowicz, A. Ziębowicz, B. Bączkowski, Solid State Phenom. **227**, 447-450 (2015).
[4] A. Ziębowicz, B. Bączkowski, Information Technologies in Biomedicine, Springer **7339**, 341-350 (2012).
[5] M. Pochrząst, J. Marcinak, M. Basiaga, W. Walke, Przeglad Elektrotechniczny **89** (12), 310-313 (2013).
[6] J. Szewczenko, M. Basiaga, M. Kiel-Jamrozik, M. Kaczmarek, M. Grygiel, Solid State Phenom. **227**, 483-486 (2015).
[7] M. Basiaga, Z. Paszenda, W. Walke, P. Karasiński, J. Marciniak, Solid State Phenom. **227**, 491-494 (2015).
[8] K-H. Kim, N. Ramaswamy, Dent. Mater. J. **28** (1), 20-36 (2009).
[9] M. Pyrliński, H. Mimanowska-Shaw, Implant protet. Stomatol. Kli. **8** (4), 50-52 (2007).
[10] M. Marędzak, A. Siudzińska, Przem. Che. **93** (6), 920-923 (2014).
[11] W. Walke, Z. Paszenda, P. Karasiński, J. Marciniak, Arch. of Mater. Sci. and Eng. **55** (2), 78-84 (2012).
[12] W. Kajzer, A. Kajzer, M. Grygiel-Pradelok, A. Ziebowicz, B. Ziebowicz, Adv. Intell. Sust. **472**, 385-398 (2016).
[13] L. Pin, F. Ansart, J.P. Bonini, Y. Le Moult, V. Vidal, P. Lours, J. Eur. Ceram. Societ. **33** (2), 269-276 (2013).
[14] PN – EN ISO 5832 – 11.
[15] B. Burnat, M. Walkowiak-Przybyło, T. Błaszczyk, L. Klimek, Acta Bioeng. Biomech. **15** (1), 87-95 (2013).
[16] Z. Paszenda, W. Walke, S. Jadacka, J. Achiev. Mater. Manuf. **38** (1), 24-32 (2010).
[17] A. Kazek-Kęsik, K. Pietryga, M. Basiaga, A. Blacha-Grzechnik, G. Dercz, I. Kalemba-Rec, E. Pamuła, W. Simka, Surf. Coat. Technol. **328**, 1-12 (2017).
[18] M. Basiaga, W. Kajzer, W. Walke, A. Kajzer, M. Kaczmarek, Mater. Sci. Eng. **68** (1), 851-860 (2016).
[19] W. Walke, M. Basiaga, Z. Paszenda, A. Kajzer, W. Kajzer, J. Szewczenko, T. Pustelny, S. Drewniak, Z. Opilski, C. Krawczyk, Surf. Coat. Technol. **307**, 753-760 (2016).
[20] J. Jaglarz, J. Szewczenko, K. Marszałek, M. Basiaga, M. Marszałek, R. Gaweł, Mater. Today-Proc. **2**, 4046-4052 (2015).